applied sciences

MDPI

Article

Investigation of a Method for Strengthening Perforated Cold-Formed Steel Profiles under Compression Loads

Ehsan Taheri [1,*], Ahmad Firouzianhaji [1], Nima Usefi [1], Peyman Mehrabi [2], Hamid Ronagh [1] and Bijan Samali [1]

[1] Centre for Infrastructure Engineering, Western Sydney University, Sydney 2747, Australia; a.firouzianhaji@westernsydney.edu.au (A.F.); n.usefi@westernsydney.edu.au (N.U.); h.ronagh@westernsydney.edu.au (H.R.); b.samali@westernsydney.edu.au (B.S.)

[2] Department of Civil Engineering, K.N. Toosi University of Technology; Tehran 15875-4416, Iran; peyman804m@gmail.com

* Correspondence: e.taheri@westernsydney.edu.au

Received: 24 October 2019; Accepted: 20 November 2019; Published: 25 November 2019

Abstract: Cold-formed steel (CFS) storage rack structures are extensively used in various industries to store products in safe and secure warehouses before distribution to the market. Thin-walled open profiles that are typically used in storage rack structures are prone to loss of stability due to different buckling modes such as local, distortional, torsional and flexural, or any interaction between these modes. In this paper, an efficient way of increasing ultimate capacity of upright frames under compression load is proposed using bolts and spacers which are added externally to the section with certain pitches along the height. Hereinto, experimental tests on 81 upright frames with different thicknesses and different heights were conducted, and the effect of employing reinforcement strategies was examined through the failure mode and ultimate load results. Non-linear finite element analyses were also performed to investigate the effect of different reinforcement spacing on the upright performance. The results showed that the reinforcement method could restrain upright flange and consequently increase the distortional strength of the upright profiles. This method can also be effective for any other light gauged steel open section with perforation. It was also observed that the reinforcement approach is much more useful for short length upright frames compared to the taller frames.

Keywords: upright; cold-formed steel; compression behavior; bolt and spacer; reinforcement

1. Introduction

By increasing the speed of development in various industries, there is a need for well-engineered warehousing systems to store the products in safe and secure warehouses before they are distributed to the market. For this purpose, cold-formed steel (CFS) storage rack structures have widely been developed to be used in different industries. Uprights are one of the main parts of the racking structures which have the important role of bearing loads like what columns do in buildings. The performance of racking frames depends on the overall behavior of the uprights, as these thin-walled structures are subjected to loss of stability due to the combination of different failure modes, such as the interaction of distortional and flexural buckling [1,2]. The stability of uprights in racking systems also becomes more critical under extreme loading scenarios [3–6].

The compressive behavior of upright racking systems has been extensively studied in recent years. Experimental tests on stub uprights and full upright frames were carried out by Koen [7] in order

to obtain a set of reduction coefficients for the effective length of the uprights under compression. Local buckling of stub column members under axial load was experimentally investigated by Davies et al. [8] and the results were compared with theoretical relations as well as the numerical method. They concluded that for the design stage of racking uprights, extensive experimental testing is not necessarily required. In another study, Trouncer and Rasmussen [9] investigated that the predicting ultimate load capacity of upright sections provided by EN 15512 [10] specification is more accurate than predictions by Rack Manufacturers Institute (RMI) specifications. Comprehensive experimental tests on individual components of racking systems were also carried out by Gilbert & Rasmussen [11], and some clarifications of the guidance provided by EN15512 [10] were presented in order to accurately determine the in-plane global stiffness of the upright frame.

The interaction of buckling modes of racking upright members has also been under the attention of researchers in recent years. The local-distortional buckling interaction in fixed-end CFS uprights was experimentally assessed by Pedro et al. [12]. In another project, local-distortional buckling interaction of short upright columns was studied by Roure et al. [13] through the concept of reduced thickness of the stiffeners. They reported that the current design codes are not accurate and the effect of buckling interaction needs to be also considered. In another study, Casafont et al. [14] experimentally evaluated the distortional buckling of upright frames with different heights and provided design formulations based on the combination of distortional and global buckling modes.

In terms of perforation, which is an important parameter that can affect the performance of upright sections under compressive load, Zhao et al. [15] investigated the effect of perforation on compressive behavior of storage rack uprights. They showed that the perforation could significantly affect the load-bearing capacity as well as buckling failure mode of the system. The influence of perforation pattern including of perforation position, dimensions, and quantity on the compressive behavior of upright frames were also assessed by Rhodes and Schneider [16]. A series of experimental tests were conducted by Moen and Schafer [17] to examine the effect of perforation on the stability behavior of upright frames. In another study [18], they indicated that direct strength method is not enough for the design of rack structures and the experimental test is also required; accordingly, the design approach for upright sections must be based on experimental test procedures. Baldassiono [19] also determined the effect of perforations and applying load on the upright strength through the axial tests on both perforated and non-perforated uprights with various length and load eccentricities.

Considering the weaknesses of the upright frames under compressive loads, in recent years several methods have been proposed in order to improve the compressive behavior of racking uprights. Partial reinforcement of open sections using spacers was proposed by Talikoti and Bajoria [20]. They concluded that by installing spacers at appropriate intervals, the capacity of the uprights is improved and the mode of failure and buckling can be changed at the same time. Veljkovic and Johansson [21] also studied the effect of partially closing CFS thin-walled sections. They focused on increasing the torsional stiffness of these sections when used as columns in structures. An investigation for analyzing the behavior of thin-walled channels with partially closed sections under axial forces using different stiffener plates was conducted by Manikandan and Arun [22]. The result indicated that by partially reinforcing the sections using cover plates, the buckling mode changes from distortional to a combination of local and flexural torsional buckling. Recently, a few studies on improving the upright axial capacity have also been carried out by other researchers [23–27] which are mainly based on numerical parametric studies.

Review of the past studies shows that a great number of research projects have been conducted on the investigation of buckling modes for CFS uprights and little attention has been given to address the weaknesses of the uprights under compressive load. Although some attempts have been made in order to increase the ultimate capacity of open CFS sections using partially closed methods, extensive experimental studies for increasing upright capacity is still required. Therefore, this study aims to propose a new approach in order to improve the strength of the uprights in racking systems and to control buckling issues using reinforcements along the upright length. The main idea is to gain

solutions that can be implemented by the industry immediately without any major modifications to the way the industry operates or to the assembly procedure. Hereinto, a total of 81 full-scale experimental tests were conducted on uprights with different heights and thicknesses in order to examine the compressive behavior and strength of upright frames with and without reinforcement. The results include the deformation modes, the failure mechanisms, and ultimate capacities, followed by a discussion on the experimental data. A finite element (FE) model was also employed to investigate the effect of different reinforcement spacing on the upright strength.

2. Reinforcement Method

Upright sections can undergo three modes of instabilities under compressive load: Local, distortional, and flexural or flexural-torsional buckling. The design of uprights is remarkably affected by distortional buckling, which has limited the applicability of thin-walled CFS profiles.

Generally, the compressive strength of open sections is significantly lower than the compressive resistance of closed sections since open sections are more prone to warping and buckling effects than closed sections. Yet, closed section production is very costly and time-consuming as the CFS industry requires a complicated procedure for providing a section in a closed-form. Therefore, increasing the capacity of upright frames can be obtained by offering a partially closed section which is more straightforward and more cost-effective. To achieve this goal, an innovative and simple approach for partially closing of upright sections was employed in this study. Using this method, the mode of failure can be controlled to have a significant change in the overall behavior of the compression element.

Each upright frame consists of a regular pattern of perforations which can be placed on both the web and the flanges. The web perforation is used for fast interconnection between beams and uprights, while the flanges' perforations allow for the connection of brace components to uprights. Those perforations which are not in use in the section can also be employed for partial closing of section. Therefore, in this study, connectors using bolts, nuts, and spacers are utilized at the location of perforations to connect the flanges of the open section, and thereafter create a partially closed section offering a higher load capacity system. Spacers are the transverse elements made up of the plastic material, which are commonly used for bracing of racking frames. Figure 1 schematically shows the proposed reinforcing method on the open CFS upright frame.

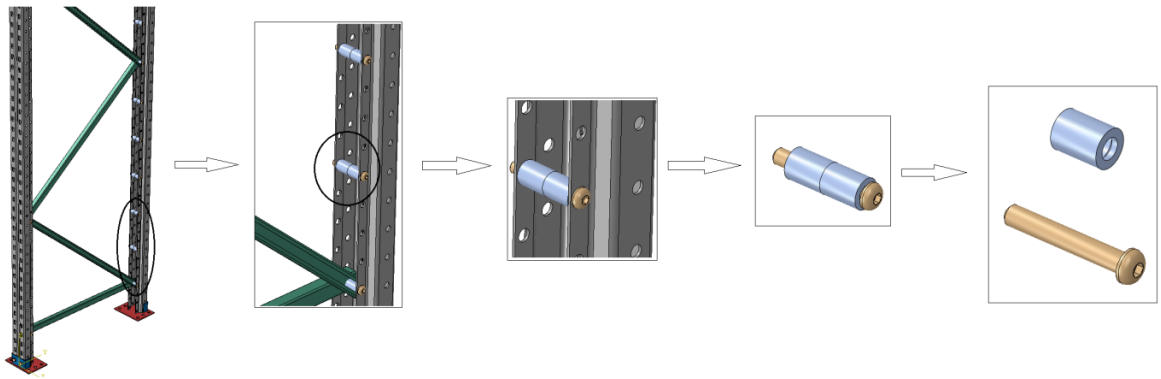

Figure 1. Schematic of the proposed reinforcing method.

It should be noted that in the racking industry, usually a single long upright is employed for the total height since it is costly and time-consuming to cut and splice the element. This strategy is uneconomical because for higher levels of racking systems, where the applied loads are low compared to those at bottom levels, the thickness of sections is considered to be the same as thickness at the lower height. In other words, the upright section is overdesigned for the higher levels which causes some economic issues. The proposed method on the other hand can be used to overcome this unnecessary steel usage. Low thick upright sections can be utilized for storage rack in which the lower level is

strengthened by the proposed method to provide higher capacity. This approach can significantly reduce the cost of making these structures.

Preliminary numerical analysis was also performed in order to check the feasibility and capability of the proposed method, and it was found that this approach can increase the load-bearing capacity of standard uprights. The reinforcement method proposed in this study is a simple, time and cost-effective approach which can be employed for many CFS open sections [28–31].

3. Experimental Test

An extensive experimental study was planned and carried out at the structural laboratory of Western Sydney University in order to investigate the effect of reinforcement on the upright capacity. Experimental tests on various upright lengths from short to long (as is used in the industry) with two different thicknesses were carried out using two scenarios of reinforcements (employing reinforcement at 200 mm and 400 mm). First, specimens without reinforcement were tested to capture the buckling strength and mode of failure of currently-in use upright frames. Then, the specimens reinforced by bolts and spacers were tested again for evaluation of the effect of the reinforced system.

3.1. Test Specimens

Nine single uprights and 72 upright frames, each comprising two upright columns attached by diagonal bracing were constructed from commercially available rack sections. The convention used for designation of specimens is explained in Figure 2.

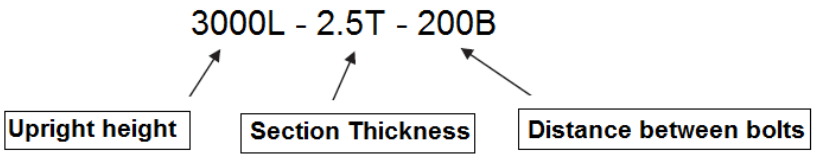

Figure 2. Designation of specimens (values in mm).

The test arrangement comprises a frame assembly with 840 mm width from the back of one upright's web to the back of the other upright's web in the frame. A standard section with two different thicknesses of 1.6 mm and 2.5 mm were utilized for the racking frames to examine the effect of thickness on the results. The geometry of the section as well as the perforation details are indicated in Figure 3. Due to commercial confidentiality reasons, all geometries are presented in non-dimensional form. In order to determine different failure modes and their corresponding interaction, different lengths of 1200 mm, 1800 mm, 2400 mm, 3000 mm, and 3600 mm were considered, as shown in Figure 4. Single upright profile was employed for 1200 mm length because of the limitation on having a full-frame with this length.

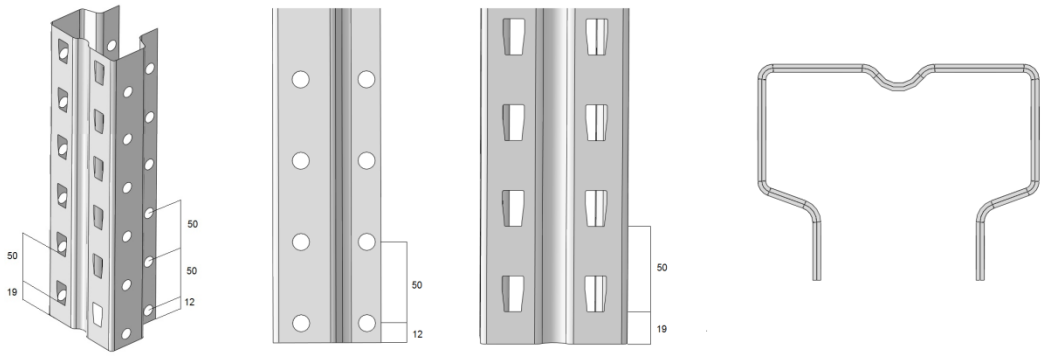

Figure 3. Section and perforation details.

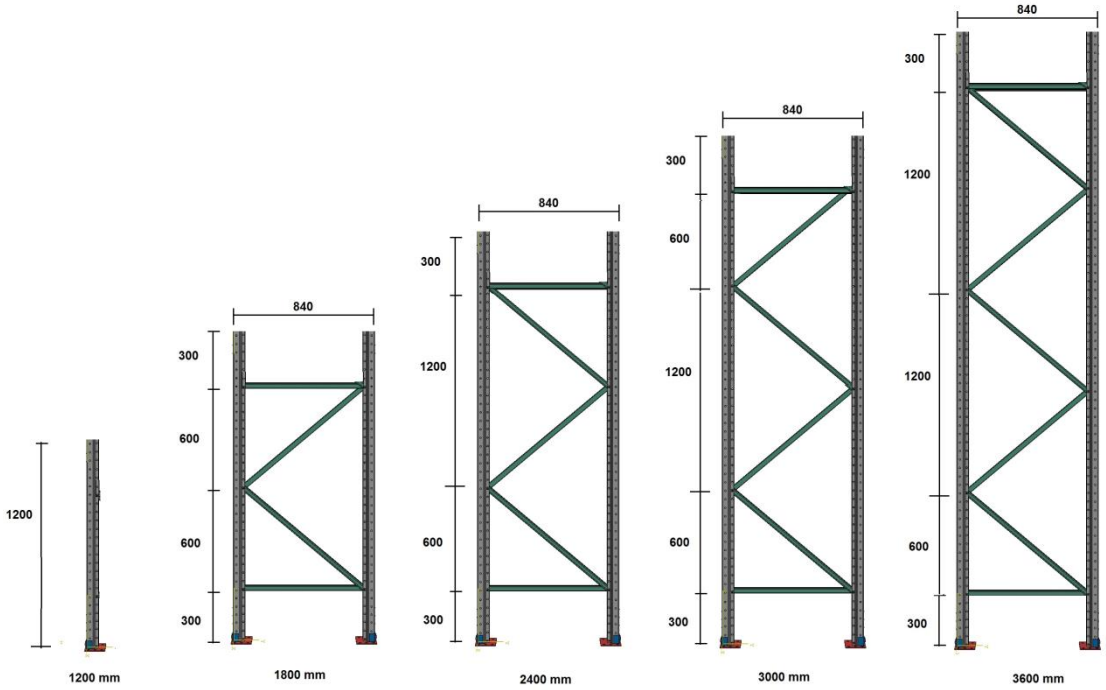

Figure 4. Schematic of specimens with different heights.

In order to evaluate the effect of reinforcement on the compressive behavior of uprights, bolts and spacers were attached to the upright at 400 mm and 200 mm space along the upright length. Figure 5 shows the example pattern of bolt and spacer attachment for reinforcing of the sections. The details of each specimen including length, thickness, and reinforcement type are also provided in Table 1.

Figure 5. Reinforcement along the upright length by bolts and spacers.

Table 1. Specimen details.

Specimen Designation	Length (mm)	Reinforcement Type	Thickness (mm)
1200L-1.6T	1200	-	1.6
1200L-1.6T-400P		@ 400 mm	
1200L-1.6T-200P		@ 200 mm	
1800L-1.6T	1800	-	
1800L-1.6T-400P		@ 400 mm	
1800L-1.6T-200P		@ 200 mm	
2400L-1.6T	2400	-	
2400L-1.6T-400P		@ 400 mm	
2400L-1.6T-200P		@ 200 mm	
3000L-1.6T	3000	-	
3000L-1.6T-400P		@ 400 mm	
3000L-1.6T-200P		@ 200 mm	
3600L-1.6T	3600	-	
3600L-1.6T-400P		@ 400 mm	
3600L-1.6T-200P		@ 200 mm	
1800L-2.5T	1800	-	2.5
1800L-2.5T-400P		@ 400 mm	
1800L-2.5T-200P		@ 200 mm	
2400L-2.5T	2400	-	
2400L-2.5T-400P		@ 400 mm	
2400L-2.5T-200P		@ 200 mm	
3000L-2.5T	3000	-	
3000L-2.5T-400P		@ 400 mm	
3000L-2.5T-200P		@ 200 mm	
3600L-2.5T	3600	-	
3600L-2.5T-400P		@ 400 mm	
3600L-2.5T-200P		@ 200 mm	

3.2. Material Properties

Tensile coupon tests were also carried out to obtain the material properties including yield stress, ultimate stress, and elongation of the specimens. Three coupon samples for each thickness were cut from the flange of the upright where there was no perforation. A 300 kN capacity MTC Sintech testing machine with a rate of 0.01 mm/s was employed for coupon tests following the AS4600 [32] procedures. Figure 6 shows the stress-strain curves for both 2.5 mm and 1.6 mm sections. The mean value of the ultimate tensile strength (σ_u), yield stress (σ_y), and elongation are also presented in Table 2.

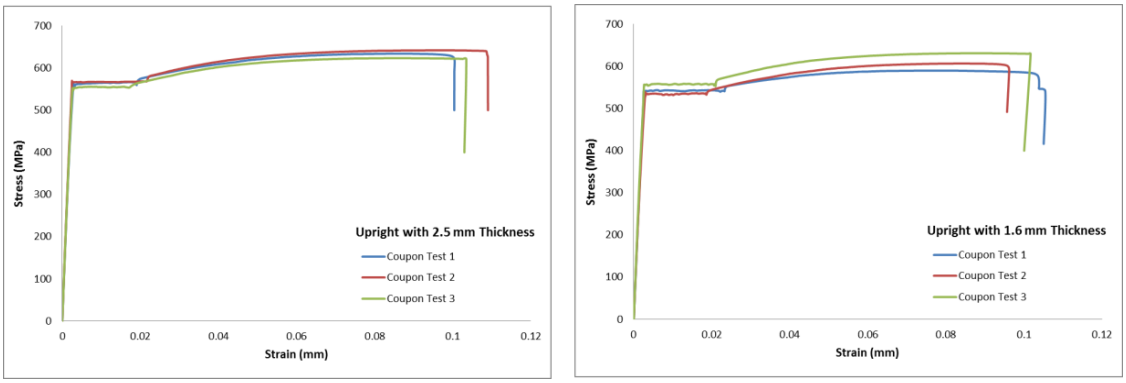

Figure 6. Coupon test results for uprights with 1.6 mm and 2.5 mm thickness.

Table 2. Material properties of upright sections.

Section Type	Yield Stress, σ_y (MPa)	Ultimate Stress, σ_u (MPa)	Elongation (%)
Uptight with 2.5 thickness	572	608	13
Uptight with 1.6 thickness	563	591	11

3.3. Test Rig and Test Setup

The test rig was prepared according to AS 4084:2012 [33] section C.7.3.2 titled: Compression tests on uprights—determination of buckling curves. The test rig includes a frame assembly in which one of the two uprights is loaded axially, as shown in Figure 7a. According to the code, the upright is loaded through ball bearings and fitted with base and cap plates. Specimens were free to rotate about both axes due to the pin-ended bearing, while rotations about the perpendicular axis, as well as torsion, were constrained by the bracing and its connection.

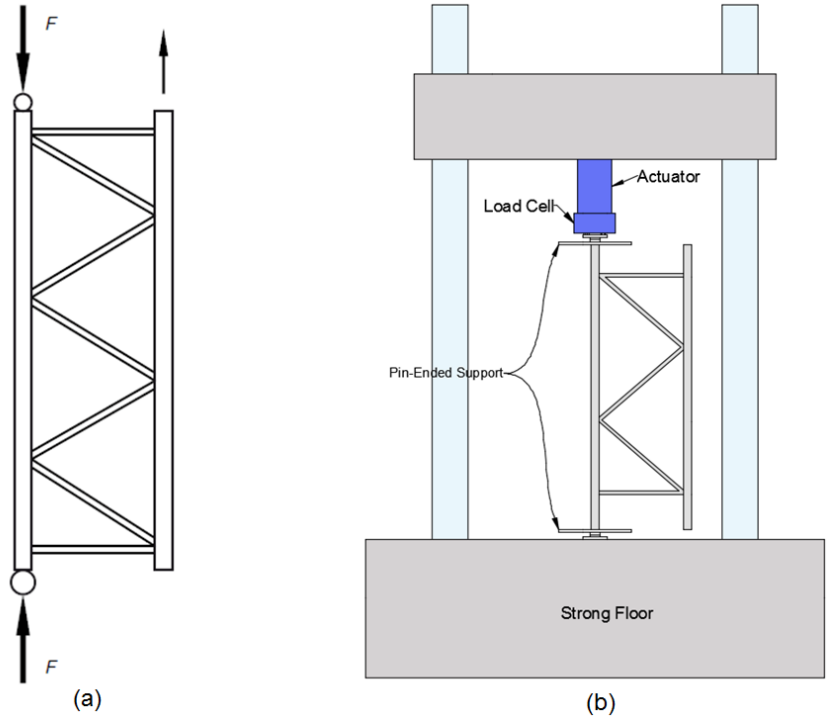

Figure 7. (**a**) Schematic of compressive test on uprights; (**b**) testing rig.

Figure 7b shows the schematic of the testing rig. The ball bearing and cap plates are also shown in Figure 8.

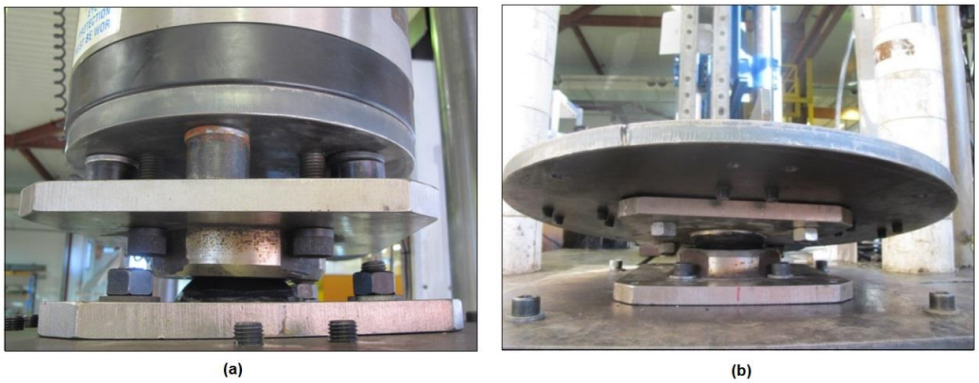

Figure 8. (**a**) Ball bearing; (**b**) cap plate.

For each test, the upright frame was assembled and positioned in the test rig between the two cap plates, which were designed to ensure uniform load distribution during the test. In order to minimize any eccentricity of loading, the upright centroid coincided with the centroid of the ball bearing. One of the uprights of each frame was loaded through hemisphere and socket joint fitted with adjustable caps, as shown in Figure 9. The upright was free to move on both ends, and the cap did not restrain it as it was not touching the upright on the sides. The other upright was connected by loose bolts to a support column. There was clearance between the support column and the whole frame in order to be free to displace and deflect laterally. Figure 10 illustrates the test setup on a typical frame (3600 mm) and depicts the support and connection system used on both ends of one upright.

Figure 9. Adjustable cap connection supports.

Figure 10. 3600 mm specimen and boundary conditions.

3.4. Test Procedure

According to the Australian Racking Code, AS4084: 2012 [33], a minimum of three tests are required for each specimen to determine the test data of each upright profile. The tests were carried out by a universal testing machine, Instron 8506 with a 3000 kN compression capacity hydraulic jack. A load cell of 500 kN capacity was also attached to the jack equipped with a linear variable differential transformer (LVDT) positioned there to record the deformation. Axial load was applied to each of the specimens using a displacement rate of 0.02 mm/s. The applying load was continued until a significant drop in the load-displacement curve of the specimens was observed.

4. Preliminary Elastic Buckling

In order to better understand the performance of a single upright member under compressive load, elastic buckling analyses for single upright with both thicknesses (1.6 mm and 2.5 mm) were conducted using the CUFSM package. Figure 11 shows the half-wavelength of sections after buckling analysis. It can be observed that for the different ranges of lengths in this study (1200 mm to 3600 mm), the dominant elastic buckling modes are distortional or flexural-torsional modes. In addition, local buckling rarely occurs in these length ranges. This paper aims to investigate the uprights of the in-use commercial rack systems. The so-called signature curves shown in Figure 11 refer to a single un-perforated profile and do not accurately predict the behavior of the perforated sections in a system. Besides, in a full upright frame, the connections at the location of bracings provide a restraint for distortional buckling which may change the buckle half-wavelength associated with the distortional buckling mode.

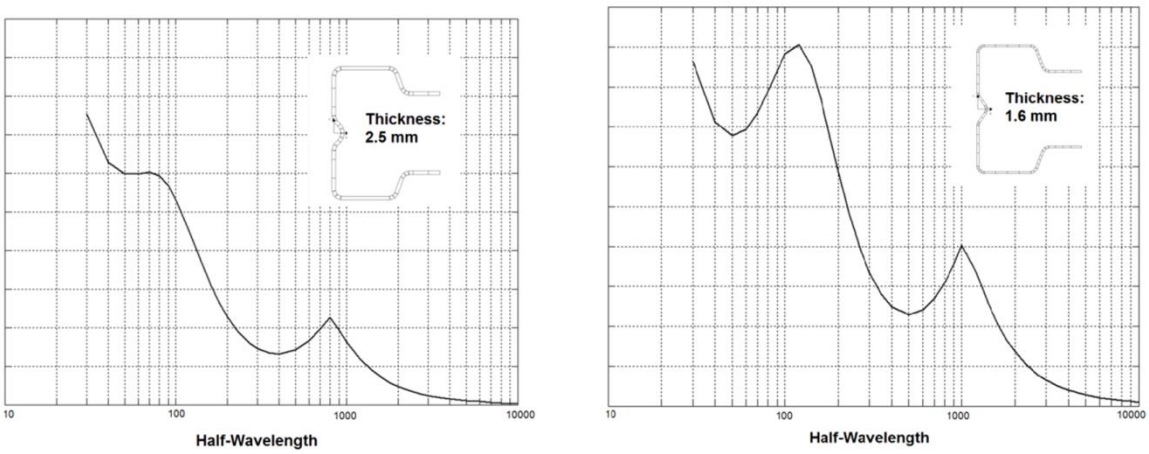

Figure 11. Preliminary elastic buckling analyses for the individual un-perforated upright gross sections (stress values have not been disclosed due to confidentiality).

It is expected that the favorable influence of the proposed reinforcement (attaching bolt and spacer) decreases by increasing the length of the element. This can be justified by the fact that the dominant mode of buckling will gradually change from distortional to flexural or flexural-torsional buckling for which the proposed reinforcement method will not be as effective.

5. Results

Compression tests were performed on the upright frames with two different thicknesses and five types of lengths, and the effect of reinforcement at 400 mm and 200 mm was investigated. Ultimate load capacities, as well as failure modes, were recorded from the compression tests and the results were accurately analyzed. At the end of the test, failure modes were investigated based on the experimental observations. For some specimens, it was relatively difficult to detect which mode of failure is dominant since the interaction of two or three buckling modes had occurred.

The ultimate load capacity of each test was extracted and normalized with respect to the gross cross-section (A_g) and the mean yielding strength (σ_y) due to the confidentiality matters. The normalized load-displacement curves of the specimens with 2.5 mm thickness are shown in Figure 12. The normalized load value is related to the compressive load applied on top of the upright, while the displacement value shows the deformation of the top head of the upright measured by LVDT. For each specimen type, at least three tests were carried out as recommended by the Australian Racking code (AS4084: 2012) [33]. The reason for the different ultimate values for these three tests of each specimen can be attributed to the fact that upright elements have different initial geometrical imperfections associated with the manufacturing processes [34].

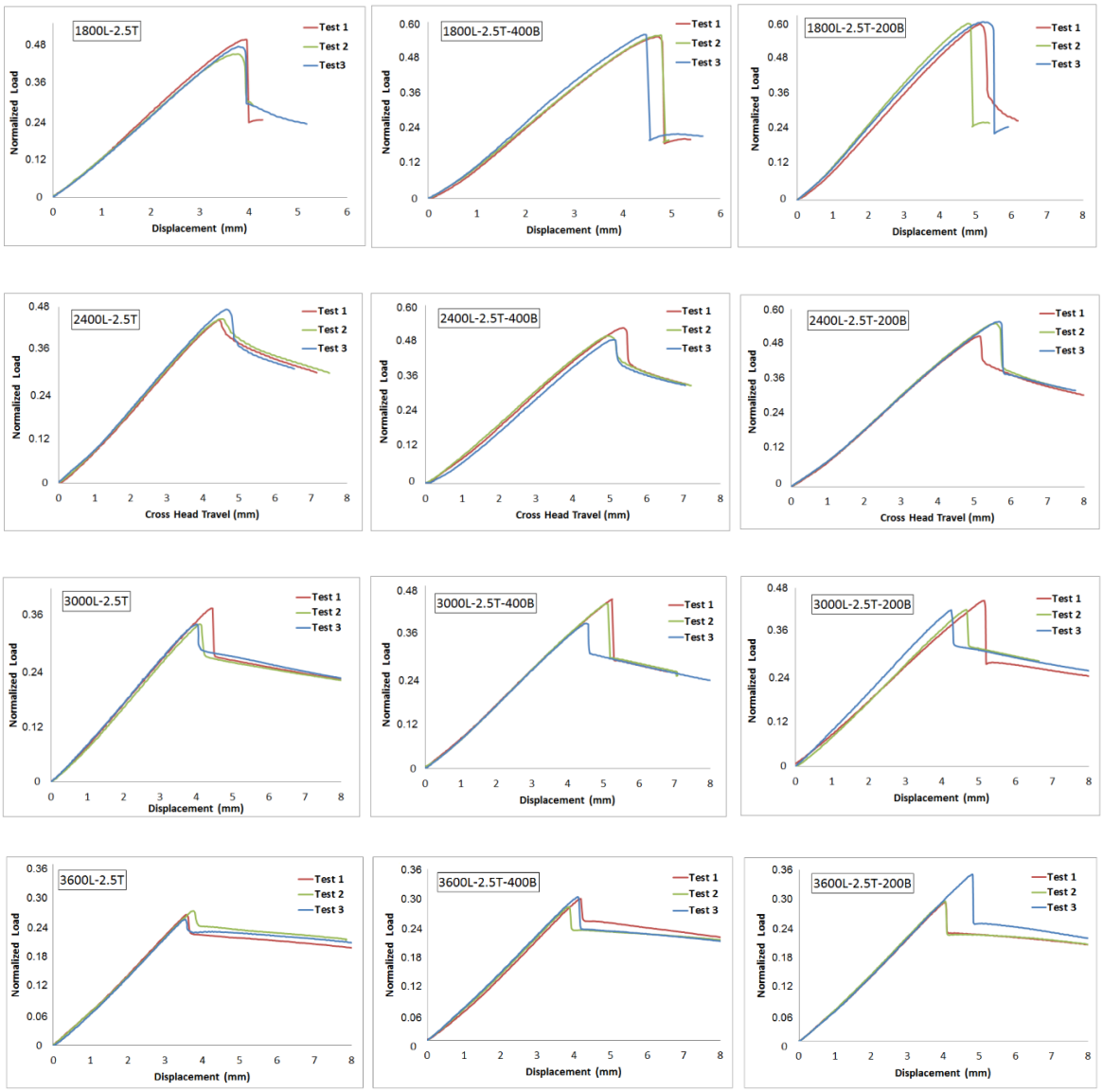

Figure 12. Load displacement curves for 2.5 mm thick specimens.

The normalized ultimate load capacity of each test, average value, and standard deviation for each specimen are provided in Table 3. In general, three types of failure modes were observed in the experimental tests: (a) Distortional buckling failure which was dominant for specimens with 1800 mm length; (b) flexural or torsional mode or combination of them was also dominant for specimens with 3000 mm and 3600 mm length; and (c) transition from distortional buckling to flexural buckling failure which happened for specimens with 2400 mm length. Local buckling was also observed in some

specimens, especially for 200 mm reinforcement pitch in which the buckle half-wavelength was limited to 200 mm.

Table 3. The average normalized ultimate capacity of uprights with 2.5 mm thickness.

Test Specimen	Normalized Buckling Load ($\frac{f}{\sigma_y \times A_g}$)		
	Without Bolt	Reinforcement at 400 mm	Reinforcement at 200 mm
1800L-2.5T-Test 1	0.478371	0.548324	0.624226
1800L-2.5T-Test 2	0.442677	0.552181	0.639532
1800L-2.5T-Test 3	0.457714	0.555499	0.615796
Ave. *	0.457385	0.550058	0.627784
Std. **	0.018176	0.004305	0.012556
2400L-2.5T-Test 1	0.443006	0.522286	0.510329
2400L-2.5T-Test 2	0.446384	0.495202	0.551224
2400L-2.5T-Test 3	0.472243	0.482437	0.556785
Ave.	0.454396	0.499238	0.538101
Std.	0.016143	0.020358	0.02541
3000L-2.5T-Test 1	0.38528	0.431019	0.445338
3000L-2.5T-Test 2	0.361663	0.422469	0.426564
3000L-2.5T-Test 3	0.360976	0.365041	0.422678
Ave.	0.370691	0.403575	0.43347
Std.	0.013751	0.035903	0.012257
3600L-2.5T-Test 1	0.270425	0.294431	0.292637
3600L-2.5T-Test 2	0.273923	0.279065	0.294879
3600L-2.5T-Test 3	0.258498	0.302233	0.350931
Ave.	0.26905	0.289976	0.310903
Std.	0.008251	0.012047	0.033093

* Average. ** Standard Deviation.

Figure 13. *Cont.*

Figure 13. *Cont.*

Figure 13. Failure modes of upright frames with 2.5 mm thickness.

According to Figure 13, the buckling mode of specimens with 3600 mm and 3000 mm, was hardly affected by employing bolts and spacers at either 200 mm or 400 mm. Therefore, it was concluded that the load capacity for specimens with and without reinforcement at higher length is not affected as significantly as shorter specimens. This is mainly because the buckling mode of failure in high length upright is governed by flexural and torsional flexural buckling, and utilizing reinforcement strategy does not necessarily change or control the buckling mode. It can be noted that one of the most effective parameters that determine the failure mode of the uprights under compression is the upright height and reinforcement might not overcome this issue.

Interestingly, for the short specimens with 1800 mm and 2400 mm length, the reinforcement system was extremely effective. Distortional buckling was the primary failure mode for these specimens and utilizing reinforcement could shorten the half-wavelength of the specimen resulting in capturing higher capacity when 400 mm and 200 mm bolts were used. The failure of the short specimens was primarily dominated by distortional buckling of the flange; while, for the taller uprights the elements were vulnerable to flexural-torsional buckling at mid-span where the uprights had low rigidity.

The effect of section thickness on the performance of an upright is considerable and should be investigated through experimental tests. Hereinto, the uprights with lower thickness were also experimentally tested in order to have a better comparison with thicker uprights. The normalized load-displacement curves of specimens with 1.6 mm thickness and their failure modes are shown in Figures 14 and 15. The average values of normalized ultimate capacity, as well as standard deviations, are also provided in Table 4. It was observed that in terms of thickness effect, as the cross-section area of this type of upright is smaller than the area of 2.5 mm thick upright, the ultimate load is significantly reduced.

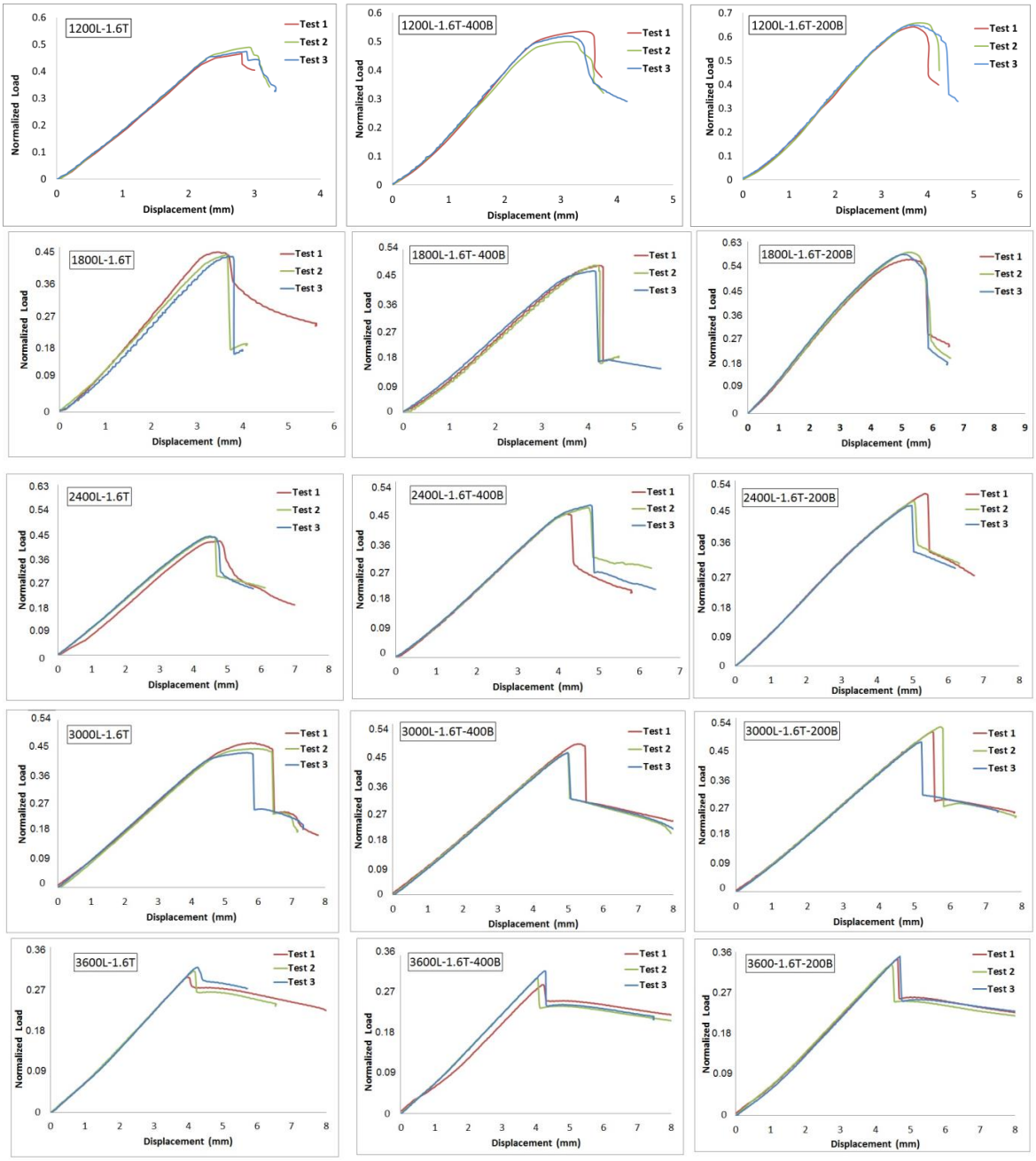

Figure 14. Load displacement curves for 1.6 mm thick specimens.

Table 4. The average normalized ultimate capacity of uprights with 1.6 mm thickness.

Test Specimen	Normalized Buckling Load ($\frac{f}{\sigma_y \times A_g}$)		
	Without Bolt	**Reinforcement at 400 mm**	**Reinforcement at 200 mm**
1200L-1.6T-Test 1	0.471698	0.54236	0.646223
1200L-1.6T-Test 2	0.483321	0.50473	0.665111
1200L-1.6T-Test 3	0.476235	0.52041	0.650512
Ave.	0.476231	0.52247	0.653952
Std.	0.005916	0.01870	0.009901
1800L-1.6T-Test 1	0.451874	0.503868	0.576726
1800L-1.6T-Test 2	0.444332	0.503357	0.610181
1800L-1.6T-Test 3	0.440257	0.485003	0.593035
Ave.	0.446066	0.497177	0.590108
Std.	0.005901	0.010733	0.017146
2400L-1.6T-Test 1	0.440072	0.454801	0.525893
2400L-1.6T-Test 2	0.450944	0.475199	0.504333
2400L-1.6T-Test 3	0.451272	0.482727	0.484913
Ave.	0.446066	0.469298	0.501824
Std.	0.006552	0.014544	0.020863
3000L-1.6T-Test 1	0.472318	0.492159	0.513533
3000L-1.6T-Test 2	0.469112	0.46586	0.533885
3000L-1.6T-Test 3	0.455033	0.468322	0.485468
Ave.	0.464652	0.473945	0.50647
Std.	0.0092	0.014637	0.024905
3600L-1.6T-Test 1	0.308389	0.303046	0.346258
3600L-1.6T-Test 2	0.320749	0.328183	0.339846
3600L-1.6T-Test 3	0.33046	0.342123	0.349139
Ave.	0.32061	0.325256	0.343842
Std.	0.011059	0.019794	0.004972

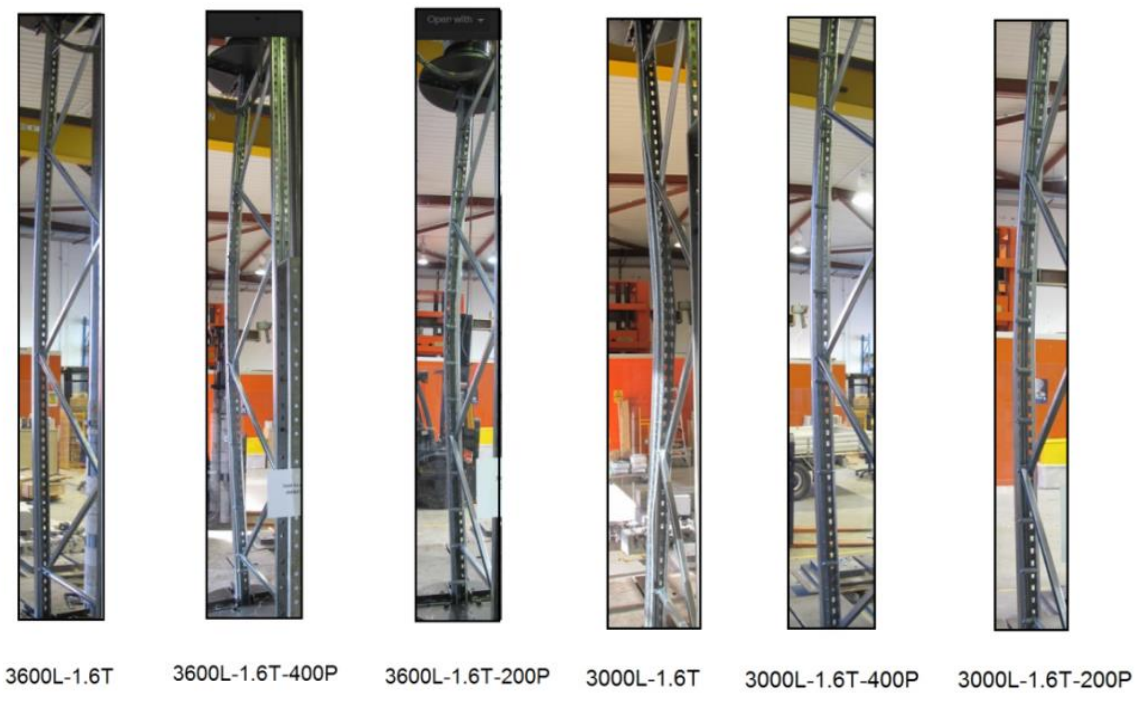

Figure 15. *Cont.*

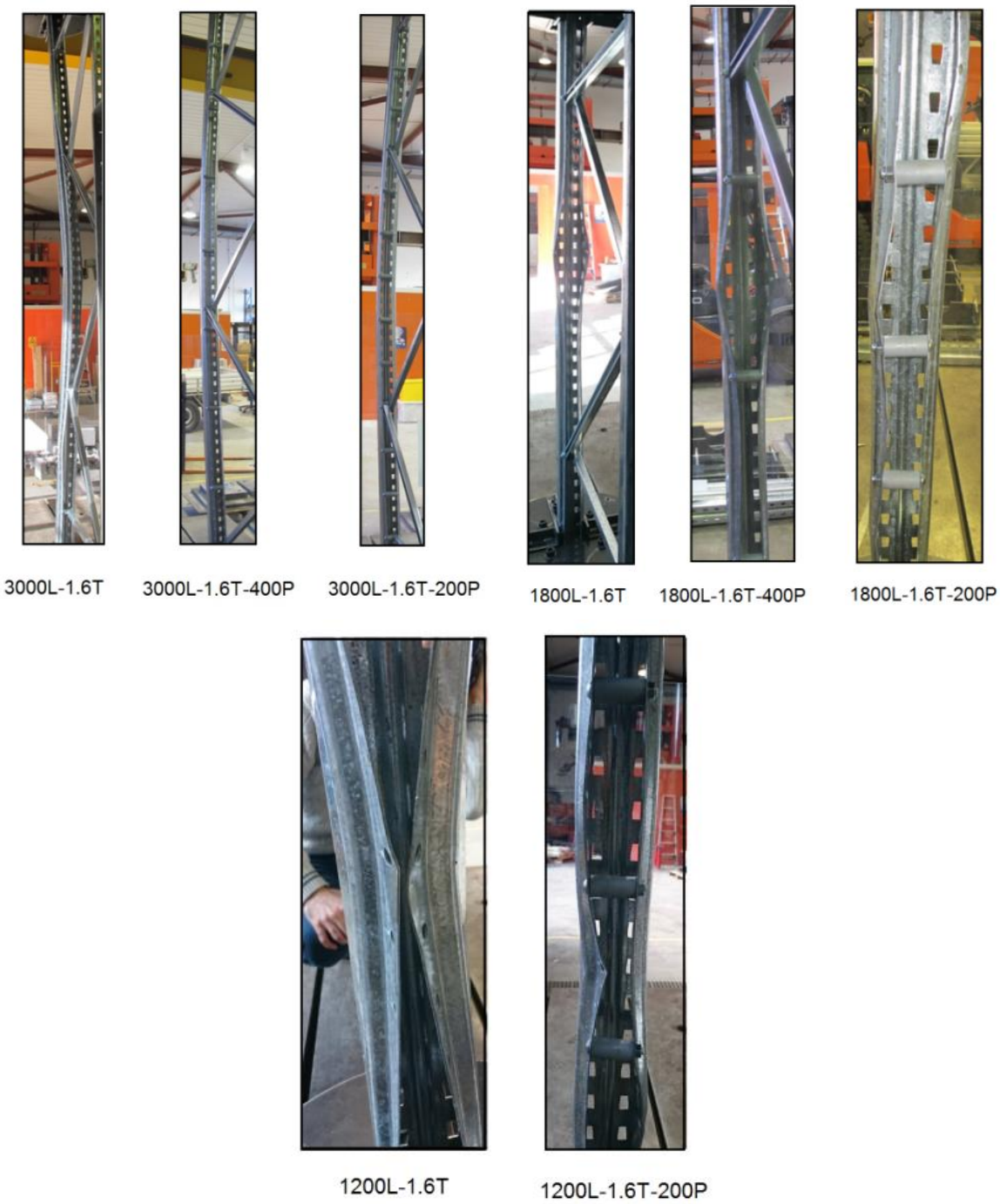

Figure 15. Failure modes of upright frames with 1.6 mm thickness.

As shown in Figures 14 and 15, the load-displacement trends and failure mode patterns for uprights with 1.6 mm thickness are somewhat similar to those observed in the tests for uprights with 2.5 mm thickness. Nevertheless, the normalized ultimate capacity for 2.5 thick upright is higher compared with the corresponding values of lower thickness uprights. For the 1.6 mm thick specimens, distortional buckling was the primary buckling failure for specimens with 1200 mm and 1800 mm length, while for the specimen with 2400 mm the failure was followed by flexural buckling or flexural-torsional buckling mode. For specimens with 3000 mm and 3600 mm length, the primary failure was flexural-torsional buckling of upright about the weak axis.

Similar to uprights with 2.5 mm thickness, the failure mode observation reveals that the reinforcement has a slight influence on the ultimate load-bearing capacity of uprights with 3000 mm

and 3600 mm and the best application of reinforcement method is for lower lengths of 1200 mm and 1800 mm due to the improvements in local and distortional buckling modes.

6. Discussion

In order to compare the capacity of different uprights, the average value of normalized ultimate loads was determined according to the test results. Figure 16 shows the normalized ultimate load capacity of uprights for both 1.6 mm and 2.5 mm thicknesses. The values of normalized ultimate loads are grouped by upright length and the type of reinforcement (bolt at 200 mm and 400 mm). As indicated in this figure, the ultimate load capacity improvement due to the reinforcement of the uprights, with different thickness and reinforcement, is decreased by increasing the upright length. This can be justified by this fact that at higher length the dominant buckling mode is flexural buckling failure mode which is not much affected by the proposed reinforcement method; therefore, increasing the ultimate capacity of the upright at higher lengths could not be achieved considerably. Figure 16 also indicates that employing bolt and spacer at 200 and 400 mm provides higher ultimate capacity compared to uprights without bolt and spacer which represents the capability of the proposed simple reinforcement method for increasing the load-bearing capacity of uprights.

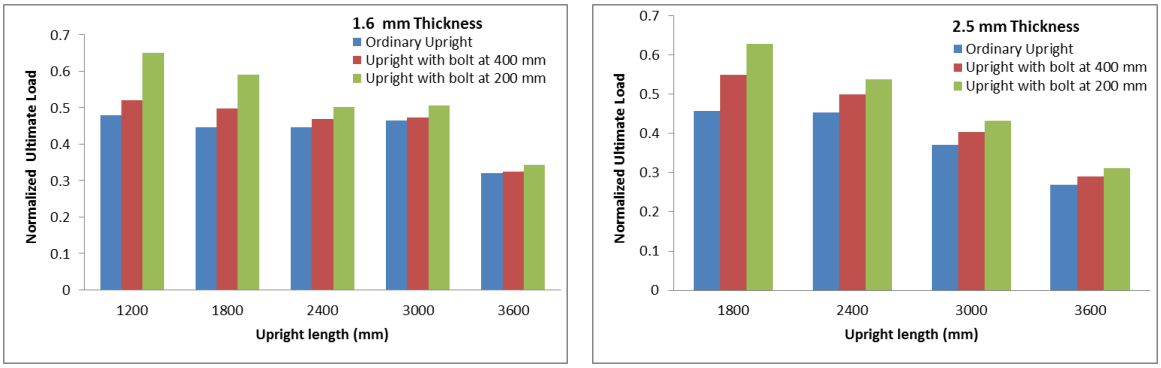

Figure 16. Comparison of normalized ultimate load capacity.

The effect of reinforcement spacing on the ultimate load capacity of uprights is also illustrated in Figure 17. As shown in this figure, a significant difference in the increase of the ultimate load capacity is observed for specimens 1800L-1.6T and 1800L-2.5T with reinforcement spacing of 200 mm compared to the 400 mm. For 1800L-1.6T upright, 33% and 12% increase in ultimate capacity resulted by employing bolts at 200 mm and 400 mm, respectively. A similar trend was also observed for 1800L-2.5T upright with 37% and 20% increase in ultimate capacity by employing bolts at 200 mm and 400 mm, respectively.

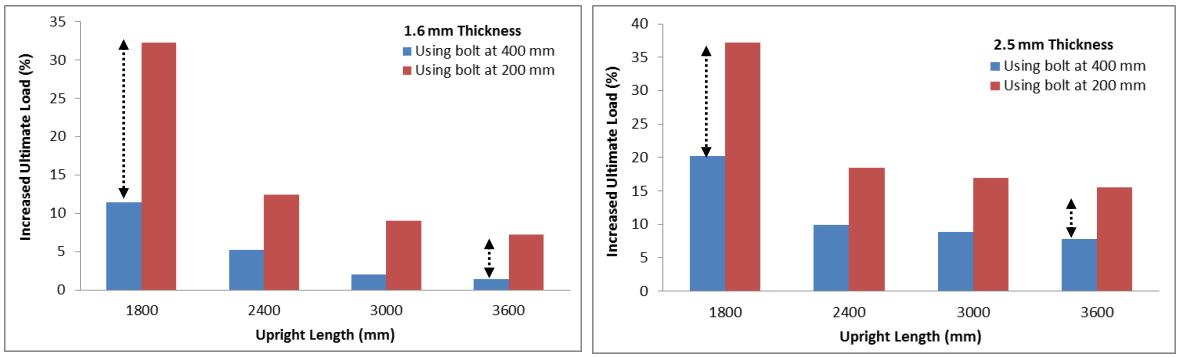

Figure 17. Effect of reinforcement by increasing the upright height.

As shown in Figure 17, the effect of employing bolt and spacer in uprights ultimate capacity is decreased by increasing the upright height. Comparing 1800L-1.6T and 3600L-1.6T specimens show that the difference between the increase in load capacity of two types of reinforcement (bolt at 400 mm and 200 mm) decreases from 23% for 1800 mm upright to 10% for 3600 mm upright. The same behavior was also captured for 2.5 mm thickness upright (1800L-2.5T and 3600L-2.5T) showing that the difference between the increased ultimate loads for the two types of reinforcement is 17% and 5% for 1800 mm and 3600 mm uprights, respectively. This indicates that the application of bolt reinforcement in shorter pitches (200 mm) in longer uprights does not offer extra resistance as much as it provides for shorter uprights since the failure of longer uprights is dominated by flexural buckling mode. Therefore, it can be concluded that although reducing the spacing of the bolts and spacers can improve the distorsional buckling capacity considerably; as discussed earlier, the effect of the reinforcement spacing on buckling mode change for higher lengths uprights is not considerable.

Figure 18 shows the effect of section thickness on the results of reinforced uprights. As shown in this figure, the reinforcement in 2.5 mm thick upright could increase the ultimate load capacity of upright much more than reinforcement in uprights with 1.6 mm thickness. A similar trend was observed in both types of uprights with 200 mm and 400 mm bolt and spacer; however, the difference between increased ultimate load for specimens with 200P is less than the difference between increased ultimate loads for specimens with 400P, for both thicknesses. In other words, when uprights were reinforced with bolts at 200 mm, the increased ultimate load percentage for 2.5 mm upright was closer to the increased ultimate load for upright with 1.6 mm compared to the other type of reinforcement (at 400 mm)

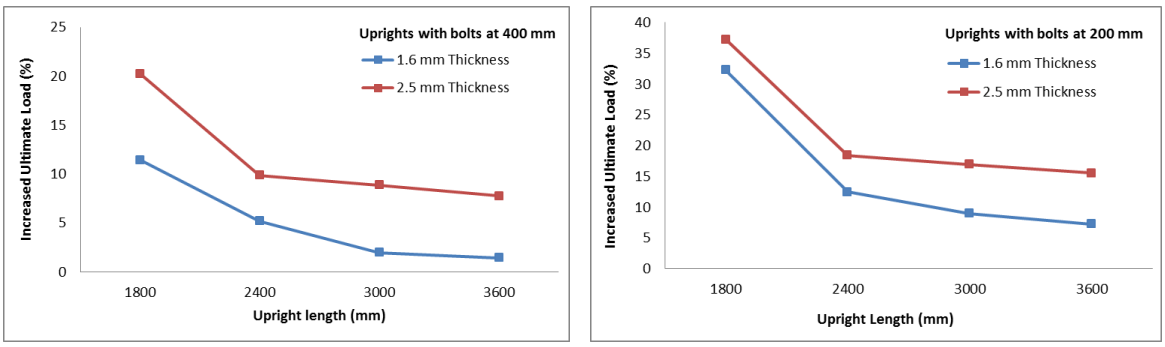

Figure 18. Effect of reinforcement on the different upright thickness.

For the 1800L-1.6T-400P and 1800L-2.5T-400P uprights, the increased ultimate load capacity was 10% and 20%, respectively. Nevertheless, the values for the condition of having bolts at 200 mm were 33% and 37% for uprights with 1.6 and 2.5 thickness. Similar behavior was observed for the other upright heights showing that the 200 mm attachment of bolts can decrease the weakness of having a low thickness section. Yet, the decrease in ultimate capacity is lower when 2.5 mm thickness section is employed. For 3600L-2.5T uprights, the application of bolts at 200 mm and 400 mm could increase the ultimate resistance by 15% and 7%, respectively; while for the same height and lower thickness (3600L-1.6T) the increased values are 7% (for bolts at 200 mm) and 3% (for bolts at 200 mm) which indicates the weakness of reinforcement for low thickness sections at high length.

According to the experimental results, it is recommended to use the reinforcement system for currently-in use racking frames in order to improve their performance under compression load. In addition, the steel tonnage of the frame and consequently, the cost of the rack system could be significantly decreased when thinner gauged sections with reinforcement are employed. It should be noted that this method is not limited to rack uprights and can also be used for any CFS C profile with flange perforations. For other CFS profiles such as L and T sections, further evaluation on the reinforcing method is required. As a future study, other reinforcement approaches can also be examined in order to find other feasible approaches for controlling torsional or flexural-torsional

buckling modes which are the dominant failure modes for long uprights. Optimization techniques can also be performed in order to determine the sufficient distance of the reinforcement with bolt and spacer [35,36].

7. Finite Element (FE) Modelling

In this paper, FE model is also employed in order to investigate the effect of other reinforcement spacing including 50 mm, 100 mm, 150 mm, 250 mm, 300 mm, and 350 mm on the strength of the upright frames. According to the experimental results, the reinforcement method was most effective for the uprights with lower height in which the distorsional buckling could significantly be controlled. Therefore, the detailed FE model with the simulation of all perforations is developed here for frames with 1800 mm height using Abaqus package [37]. First, the numerical method is well presented in details and then verified against the experimental data provided in Section 5. Finally, the effect of the different reinforcement spacing is assessed through the validated numerical model.

7.1. Material Properties

The stress-strain data from the coupon tests were utilized for the simulation of the material properties. In order to account the necking phenomena during the coupon tests, the true stress-strain relationship was employed for the numerical models [38,39]. The true stress (σ_{true}) and true strain (ε_{true}) can be obtained using the following equations:

$$\sigma_{true} = \sigma(1 + \varepsilon) \tag{1}$$

$$\varepsilon_{true} = \ln(1 + \varepsilon) - \frac{\sigma_{true}}{E} \tag{2}$$

where σ and ε are the stresses and strains obtained from the coupon tests. The von Mises yield criteria with isotropic hardening were also considered for the simulation. In addition, the Poisson ratio and the module of elasticity were assumed equal to 200 GPa and 0.3, respectively.

7.2. Connections and Interactions

Generally, two types of interactions need to be defined for the numerical model of upright frames under compression load: (a) The interaction between the upright flange edges and bracing web, and (b) the interaction between the webs of two braces at the location of the bolt connections. The surface to surface interaction with hard contact for normal behavior, as well as penalty method with the friction coefficient of 0.3 for the tangential behavior were adopted for model interactions. Coupling method and beam connectors were also utilized for modelling of the bolts. At each bolt location, a reference point was created at the center of the hole where the upright flange (at the hole region) was restrained to this reference point using the coupling method [37]. Then the reference points at two opposite sides of the uptight section were connected to each other using a beam connector. This type of connector constrains the axial translational degree of freedom between connecting nodes, simulating the actual bolt behavior in the upright frame. Figure 19 shows the interaction between frame elements as well as the modelling of the bolt in the upright frame.

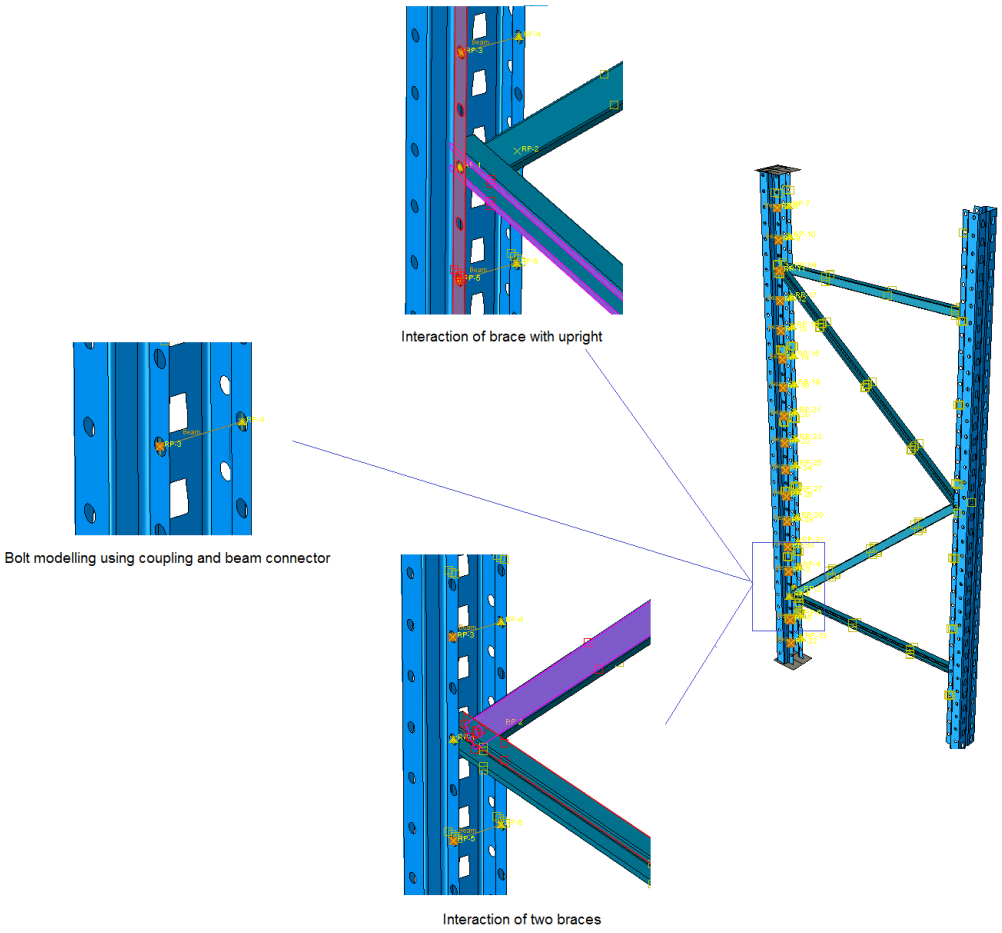

Figure 19. Interaction of the frame elements as well as bolt modelling.

7.3. Boundary Conditions and Loading

Similar to the experimental test, the pinned-end condition was also adopted for modelling of the upright frame. All element edges at the top and bottom of the upright were constrained to a reference point at the cross-section neutral axis with coupling method in order to simulate the center of the ball bearings. This means that all the displacements of the cross-section at the end are tied to the centroid by coupling constraint. The concentrated load with displacement method was applied at the top reference point. At the other end of the upright, all three translations together were restrained (Ux = Uy = Uz = 0), while the rotations about the maximum and minimum moment of inertia axes were allowed to simulate the actual test conditions.

7.4. Mesh

Shell elements were employed in this study since the thickness of the open CFS members is very small compared to their width and length; thus, buckling deformations could be explicitly modelled [37,40]. The four-noded shell element with reduced integration (S4R) was utilized for modelling of the frame elements. Convergence study was performed to capture the optimum mesh size for the upright and bracing members and it was observed that quad dominated meshes with dimensions of 10 mm were deemed satisfactory for frame elements. The final mesh used for the upright models is shown in Figure 20.

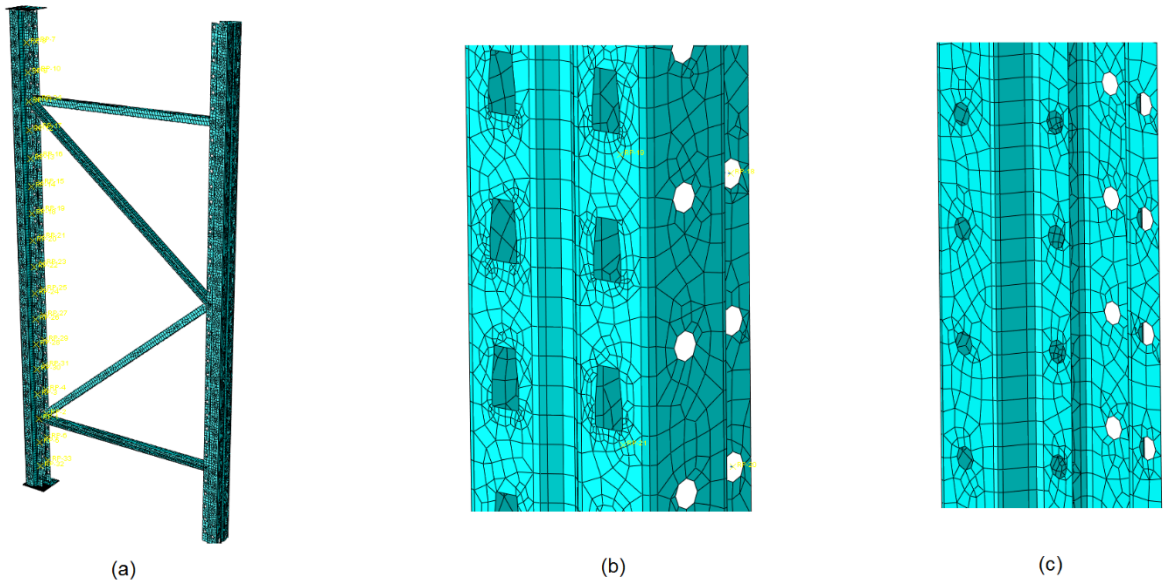

Figure 20. (**a**) Full frame meshing, (**b**) meshing around the polygon perforations, and (**c**) meshing around the circular perforations.

7.5. Validation of the FE Model

Experimental results obtained from upright with 1800 mm height for both thicknesses were used to evaluate the validity and accuracy of the numerical model. Figures 21 and 22 show the comparisons between the numerical and test results in terms of load-displacement curves for uprights with 1.6 mm and 2.5 mm thickness, respectively. As indicated in these figures, the developed FE model predicts well the overall load-displacement curve of the specimens. The slight differences between the numerical and the experimental results can be attributed to this point that the load in the actual test could not precisely be applied at the centroid of the section which can cause a different eccentricity compared to numerical inputs.

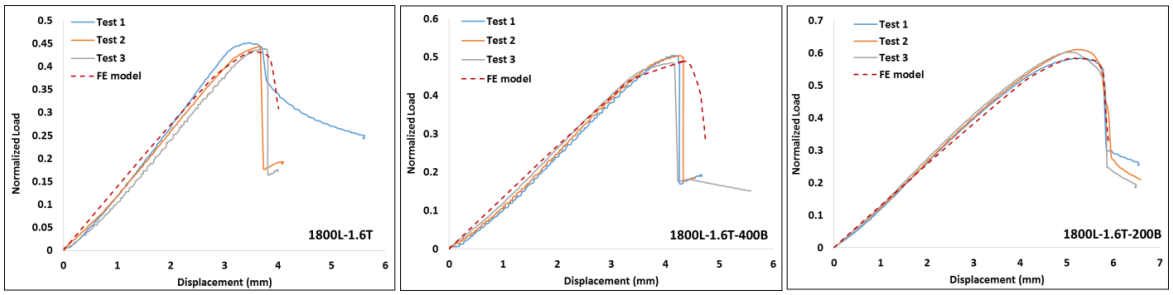

Figure 21. Comparison of the finite element (FE) model against the experimental data for 1.6 mm thick uprights.

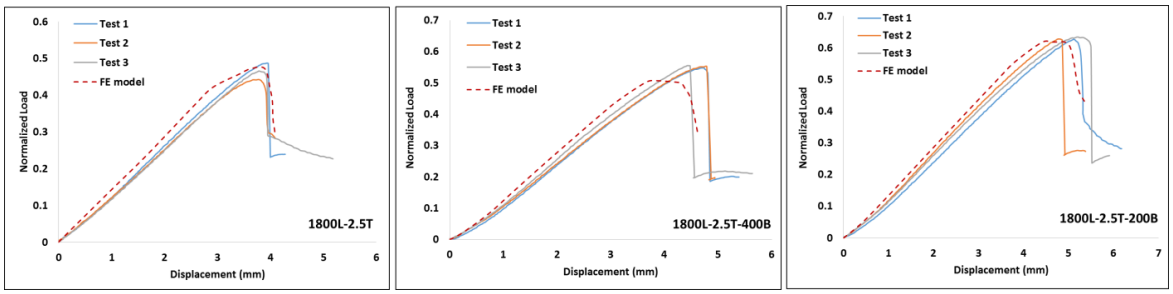

Figure 22. Comparison of the FE model against the experimental data for 2.5 mm thick uprights.

Figure 23 also illustrates the final deformation of uprights for both numerical model and experimental test. Similar to the experimental deformations, the figure shows that the FE method is able to capture the overall behavior of the upright frames.

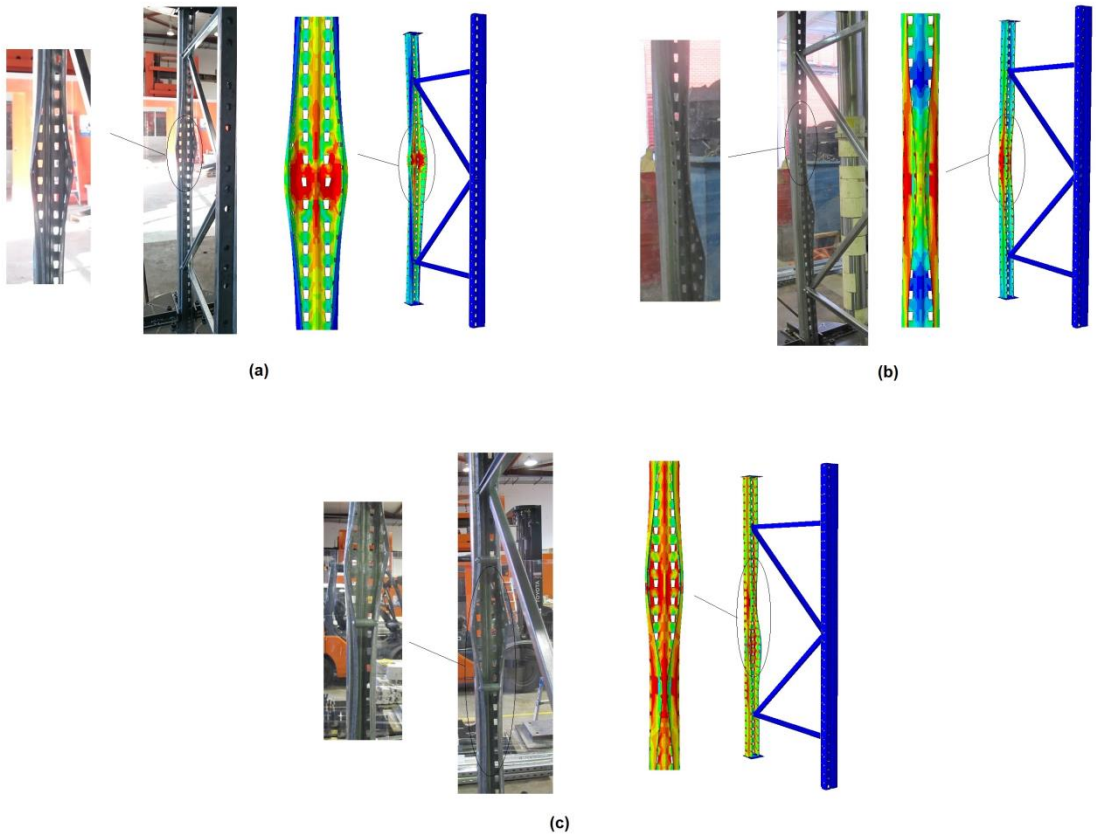

Figure 23. Comparison of failure modes, (**a**) 1800L-1.6T, (**b**)1800L-2.5T, (**c**)1800L-1.6T-400B.

Comparing FE and experimental results in terms of the load-displacement curve and deformation contours shows that the FE model is capable of estimating the overall behavior of the upright frame. Therefore, the numerical modelling is reliable enough to undertake a further study for investigating the effects of different reinforcement spacing on the buckling behavior of uprights.

7.6. Effect of Different Reinforcement Spacing

Overall, eight different reinforcement spacing including 50 mm, 100 mm, 150 mm, 200 mm, 250 mm, 300 mm, 350 mm, and 400 mm were considered for the parametric study. Due to the location of the perforations, the spacing allocation was limited to 50 mm intervals. The numerical analyses were performed for both 1.6 mm and 2.5 mm thick upright frames and the results were compared with each other. Figure 24 shows the normalized load-displacement curves of the numerical models for both thicknesses. It can be observed that, employing more reinforcement to partially close the section leads to increase in the strength of the upright, which means that reinforcement should be taken into account, especially for uprights with a shorter length.

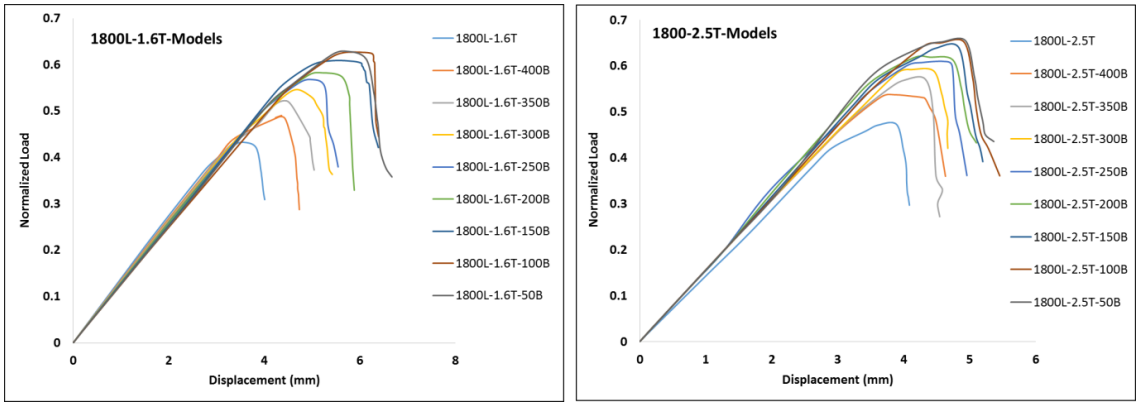

Figure 24. Load-displacement curves of uprights with different reinforcement spacing.

The normalized ultimate strength of the uprights with different reinforcement spacing is also represented in Figure 25. From this figure, it is concluded that by employing shorter reinforcement spacing, the ultimate strength of the sections increases, which may contribute to the reduction in the buckling length of the section and enhancement of load sharing between the bolts. In fact, the distortional buckling behavior is improved, and section failure is changed from distortional buckling to overall buckling mainly due to partial closing of the upright section. A similar outcome is observed for both thicknesses in which increasing the number of reinforcement improves the ultimate strength of the upright for both the type of sections.

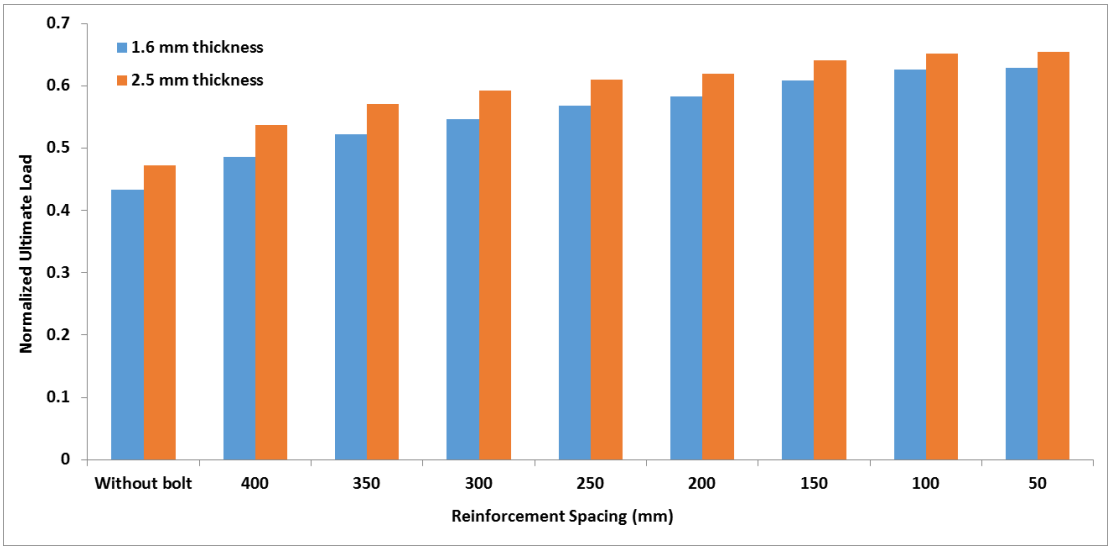

Figure 25. The normalized ultimate load of uprights with different reinforcement ratio.

Figure 26 also shows the percentage of increased ultimate strength using different reinforcement spacing in respect to upright without reinforcement condition. Generally, the reinforcement method could have a reasonable effect on the ultimate capacity of the upright frame through increasing its capacity to the range 10% to 45%. As indicated in this figure, the addition of reinforcement from 400 mm spacing to 50 mm spacing can enhance the frame's strength around 35% and 40% for uprights with 1.6 and 2.5 thicknesses, respectively. It is also shown that up to 100 mm reinforcement spacing, decreasing the reinforcement spacing can noticeably increase the ultimate strength of the upright under compression load; however, less difference in increased ultimate load is observed when reinforcement spacing decreased from 100 mm to 50 mm.

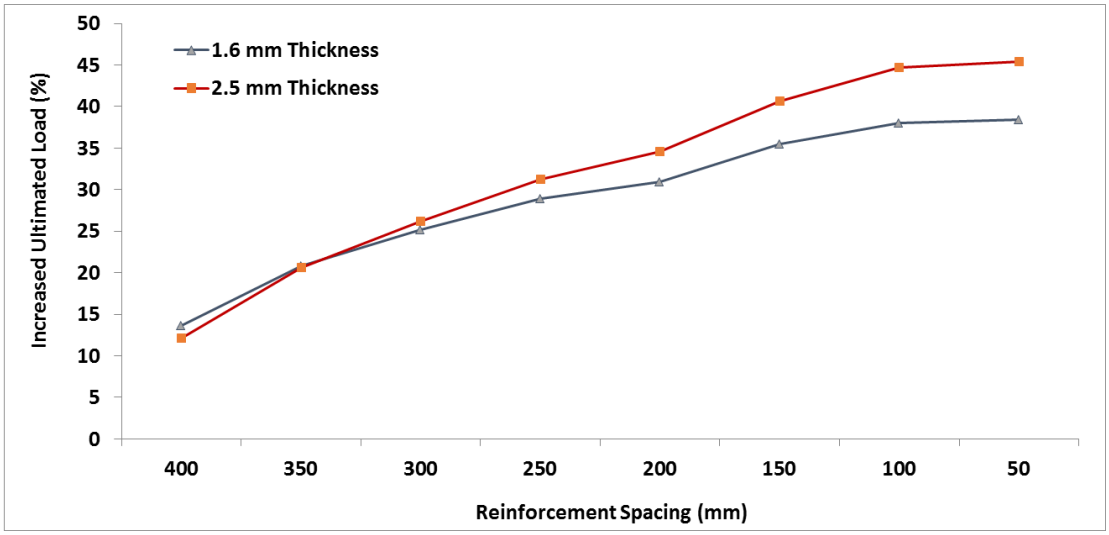

Figure 26. Percentage of increased ultimate load with different reinforcement spacing.

8. Conclusions

This study investigated the effect of a proposed reinforcement method on the compressive performance of upright frames. An extensive experimental program was conducted on 75 upright frames, and 9 single uprights with different thicknesses and heights, and the corresponding results obtained from the tests were analyzed. The reinforcement system was proposed in such a way that bolts and spacers were attached along the upright height. Experimental tests showed that the application of the reinforcement system is significantly effective for increasing the load-bearing capacity when distortional buckling failure mode governs. However, the application of this method is not particularly useful for taller frames. This justifies the fact that this reinforcing method (i.e., using bolts and spacers to partially close off the open profile) is predominantly effective on distortional buckling mode and has minimal effect on other buckling modes (torsional, flexural/torsional, local, and flexural). In addition, compared to thinner uprights (1.6 mm thick), thicker uprights (2.5 mm thick) showed higher capacity improvement (percentage of increased load compared to unreinforced frame) when reinforced with bolts and spacers. The results also showed that the reinforcement has a significant influence not only on the ultimate load capacity but also on the buckling failure mode of low length upright frames (1200 mm, 1800 mm, and 2400 mm). Numerical simulation was also employed in order to investigate the effect of different reinforcement spacing on the performance of the upright frame. It was indicated that up to 100 mm reinforcement spacing, decreasing the reinforcement spacing can increase the ultimate strength of the upright under compression load; while less improvement was observed when reinforcement spacing decreased from 100 mm to 50 mm.

Further experimental and theoretical attempts are required in order to better understand the behavior of open perforated profiles reinforced with bolts and spacers as well as other materials. Finite element method is also needed for a parametric study of different types of reinforcement systems.

Author Contributions: E.T., A.F., H.R. and B.S. devised the project, the main conceptual ideas and proof outline. E.T., A.F. and B.S. conceived and planned the experiments. E.T., A.F. carried out the experiments. E.T., A.F., N.U. and P.M. planned and carried out the simulations. E.T., A.F. contributed to sample preparation. E.T., A.F., N.U., P.M., H.R. and B.S. contributed to the interpretation of the results. N.U. and E.T. took the lead in writing the manuscript. All authors provided critical feedback and helped shape the research, analysis and manuscript.

Funding: The research was funded from R&D contract budget of Western Sydney University. The materials for laboratory testing was provided by Dexion Australia.

Acknowledgments: The authors would like to acknowledge the contribution by Dexion Australia in supporting this study.

Conflicts of Interest: The authors declare no conflict of interest.

References

1. Yang, N.; Bai, F. Damage Analysis and Evaluation of Light Steel Structures Exposed to Wind Hazards. *Appl. Sci.* **2017**, *7*, 239. [CrossRef]
2. Sharafi, P.; Mortazavi, M.; Usefi, N.; Kildashti, K.; Ronagh, H.; Samali, B. Lateral force resisting systems in lightweight steel frames: Recent research advances. *Thin-Walled Struct.* **2018**, *130*, 231–253. [CrossRef]
3. Javidan, M.M.; Kang, H.; Isobe, D.; Kim, J. Computationally efficient framework for probabilistic collapse analysis of structures under extreme actions. *Eng. Struct.* **2018**, *172*, 440–452. [CrossRef]
4. Ahmadi, R.; Rashidian, O.; Abbasnia, R.; Nav, F.M.; Usefi, N. Experimental and numerical evaluation of progressive collapse behavior in scaled RC beam-column subassemblage. *Shock Vib.* **2016**, *2016*, 3748435. [CrossRef]
5. Shayanfar, M.A.; Javidan, M.M. Progressive Collapse-Resisting Mechanisms and Robustness of RC Frame–Shear Wall Structures. *J. Perform. Constr. Facil.* **2017**, *31*, 04017045. [CrossRef]
6. Javidan, M.M.; Kim, J. Variance-based global sensitivity analysis for fuzzy random structural systems. *Comput. Aided Civ. Infrastruct. Eng.* **2019**, *34*, 602–615. [CrossRef]
7. Koen, D.J. *Structural Capacity of Light Gauge Steel Storage Rack Uprights*; University of Sydney: Sydney, Australia, 2008.
8. Michael Davies, J.; Leach, P.; Taylor, A. The design of perforated cold-formed steel sections subject to axial load and bending. *Thin-Walled Struct.* **1997**, *29*, 141–157. [CrossRef]
9. Trouncer, A.N.; Rasmussen, K.J.R. Flexural–torsional buckling of ultra light-gauge steel storage rack uprights. *Thin-Walled Struct.* **2014**, *81*, 159–174. [CrossRef]
10. Standard, B. Steel static storage systems—Adjustable pallet racking systems—Principles for structural design. *BS EN* **2009**, *15512*, 15512.
11. Gilbert, B.P.; Rasmussen, K.J.R. Bolted moment connections in drive-in and drive-through steel storage racks. *J. Constr. Steel Res.* **2010**, *66*, 755–766. [CrossRef]
12. Dinis, P.B.; Young, B.; Camotim, D. Strength, interactive failure and design of web-stiffened lipped channel columns exhibiting distortional buckling. *Thin-Walled Struct.* **2014**, *81*, 195–209. [CrossRef]
13. Roure, F.; Pastor, M.M.; Casafont, M.; Somalo, M.R. Stub column tests for racking design: Experimental testing, FE analysis and EC3. *Thin-Walled Struct.* **2011**, *49*, 167–184. [CrossRef]
14. Casafont, M.; Pastor, M.M.; Roure, F.; Peköz, T. An experimental investigation of distortional buckling of steel storage rack columns. *Thin-Walled Struct.* **2011**, *49*, 933–946. [CrossRef]
15. Zhao, X.; Ren, C.; Qin, R. An experimental investigation into perforated and non-perforated steel storage rack uprights. *Thin-Walled Struct.* **2017**, *112*, 159–172. [CrossRef]
16. Rhodes, J.; Schneider, F.D. *The Compressional Behaviour of Perforated Elements*; University of Missouri-Rolla: Saint Louis, MO, USA, 1994.
17. Moen, C.D.; Schafer, B.W. Experiments on cold-formed steel columns with holes. *Thin-Walled Struct.* **2008**, *46*, 1164–1182. [CrossRef]
18. Moen, C.D.; Schafer, B.W. Elastic buckling of cold-formed steel columns and beams with holes. *Eng. Struct.* **2009**, *31*, 2812–2824. [CrossRef]
19. Baldassino, N.; Hancock, G. Distortional Buckling of Cold-Formed Steel Storage Rack Section including Perforations. In Proceedings of the 4th International Conference on Steel and Aluminum Structures, Espoo, Finland, 20–23 June 1999.
20. Talikoti, R.; Bajoria, K. New approach to improving distortional strength of intermediate length thin-walled open section columns. *Electron. J. Struct. Eng.* **2005**, *5*, 69–79.
21. Veljkovic, M.; Johansson, B. Thin-walled steel columns with partially closed cross-section: Tests and computer simulations. *J. Constr. Steel Res.* **2008**, *64*, 816–821. [CrossRef]
22. Manikandan, P.; Arun, N. Behaviour of Partially Closed Stiffened Cold-Formed Steel Compression Member. *Arab. J. Sci. Eng.* **2016**, *41*, 3865–3875. [CrossRef]
23. Anbarasu, M.; Amali, D.; Sukumar, S. New approach to improve the distortional strength of intermediate length web stiffened thin walled open columns. *KSCE J. Civ. Eng.* **2013**, *17*, 1720–1727. [CrossRef]
24. Anbarasu, M.; Kumar, S.B.; Sukumar, S. Study on the effect of ties in the intermediate length cold formed steel (CFS) columns. *Struct. Eng. Mech.* **2013**, *46*, 323–335. [CrossRef]

25. Anbarasu, M.; Sukumar, S. Effect of connectors interaction in behaviour and ultimate strength of intermediate length cold formed steel open columns. *Asian J. Civ. Eng. (BHRC)* **2013**, *14*, 305–317.
26. Anbarasu, M.; Sukumar, S. Finite Element-Based Investigation on Performance of Intermediate Length Thin-walled Columns with Lateral Stiffeners. *Arab. J. Sci. Eng.* **2014**, *39*, 6907–6917. [CrossRef]
27. Anbarasu, M.; Sukumar, S. Influence of Spacers on Ultimate Strength of Intermediate Length Thin walled Columns. *Steel Compos. Struct. Int. J.* **2014**, *16*, 437–454. [CrossRef]
28. Ye, J.; Jiang, L.; Wang, X. Seismic Failure Mechanism of Reinforced Cold-Formed Steel Shear Wall System Based on Structural Vulnerability Analysis. *Appl. Sci.* **2017**, *7*, 182. [CrossRef]
29. Ye, J.; Wang, X. Piecewise Function Hysteretic Model for Cold-Formed Steel Shear Walls with Reinforced End Studs. *Appl. Sci.* **2017**, *7*, 94. [CrossRef]
30. Usefi, N.; Sharafi, P.; Ronagh, H. Numerical models for lateral behaviour analysis of cold-formed steel framed walls: State of the art, evaluation and challenges. *Thin-Walled Struct.* **2019**, *138*, 252–285. [CrossRef]
31. Shafaei, S.; Ronagh, H.; Usefi, N. Experimental evaluation of CFS braced-truss shear wall under cyclic loading. In *Advances in Engineering Materials, Structures and Systems: Innovations, Mechanics and Applications, Proceedings of the 7th International Conference on Structural Engineering, Mechanics and Computation (SEMC 2019), Cape Town, South Africa, 2–4 September 2019*; CRC Press: Boca Raton, FL, USA, 2019.
32. Hancock, G.J. *Design of Cold-formed Steel Structures: To Australian/New Zealand Standard AS/NZS 4600: 1996*; Institute of Steel Construction: Sydney, Australian, 1998.
33. AS 4084. *Steel Storage Racking*; Standards Australia: Sydney, Australia, 2012.
34. Shen, Y.; Chacón, R. Effect of Uncertainty in Localized Imperfection on the Ultimate Compressive Strength of Cold-Formed Stainless Steel Hollow Sections. *Appl. Sci.* **2019**, *9*, 3827. [CrossRef]
35. Kaveh, A.; Vaez, S.R.H.; Hosseini, P.; Fathali, M.A. A New Two-Phase Method for Damage Detection in Skeletal Structures. *Iran. J. Sci. Technol. Trans. Civ. Eng.* **2019**, *43*, 49–65. [CrossRef]
36. Kaveh, A.; Vaez, S.H.; Hosseini, P. Simplified dolphin echolocation algorithm for optimum design of frame. *Smart Struct. Syst.* **2018**, *21*, 321–333.
37. Abaqus, V. *6.14 Documentation*; Dassault Systemes Simulia Corporation: Johnston, RI, USA, 2014; Volume 651.
38. Usefi, N.; Ronagh, H.R.; Mohammadi, M. Finite element analysis of hybrid cold-formed steel shear wall panels. In *Streamlining Information Transfer between Construction and Structural Engineering, Proceedings of the Fourth Australasia and South-East Asia Structural Engineering and Construction Conference*; ISEC Press: Brisbane, Australia, 2018.
39. Cardoso, F.S.; Rasmussen, K.J. Finite element (FE) modelling of storage rack frames. *J. Constr. Steel Res.* **2016**, *126*, 1–14. [CrossRef]
40. Usefi, N.; Ronagh, H.; Kildashti, K.; Samali, B. Macro/micro analysis of cold-formed steel members using ABAQUS and OPENSEES. In *Volume of Abstracts, Proceedings of the 13th International Conference on Steel, Space and Composite Structures (SS18)*; The University of Western Australia: Perth, Australia, 2018.